

Flow at the SPS and RHIC as a Quark-Gluon Plasma Signature

D. Teaney, J. Lauret, E.V. Shuryak

Department of Physics and Astronomy

State University of New York, Stony Brook, NY 11794-3800

(December 2, 2024)

Radial and elliptic flow in non-central heavy ion collisions can constrain the effective Equation of State(EoS) of the excited nuclear matter. To this end, a model combining relativistic hydrodynamics and a hadronic transport code(RQMD [17]) is developed. For an EoS with a first order phase transition, the model reproduces both the radial and elliptic flow data at the SPS. With the EoS fixed from SPS data, we quantify predictions at RHIC where the Quark Gluon Plasma(QGP) pressure is expected to drive additional radial and elliptic flow. Currently, the strong elliptic flow observed in the first RHIC measurements does not conclusively signal this nascent QGP pressure. Additional measurements are suggested to pin down the EoS.

1. By colliding heavy nuclei at the SPS and RHIC accelerating facilities, physicists hope to excite hadronic matter into a new phase consisting of deconfined quarks and gluons – the Quark Gluon Plasma(QGP) [1]. After the collision, the produced particles move collectively or *flow* and this flow may quantify the effective Equation of State(EoS) of the matter. In central PbPb collisions at the SPS, a strong radial flow is observed [2]. The matter develops a collective transverse velocity approaching $(1/2)c$. In non-central collisions, a radial and an *elliptic* flow are observed [3–5]. Since in non-central collisions the initial nucleus-nucleus overlap region has an elliptic shape, the initial pressure gradient is larger along the impact parameter and the matter moves preferentially in this direction [6].

The phase transition to the QGP influences both the radial and elliptic flows. QCD lattice simulations show an approximately 1st order phase transition [7]. Over a wide range of energy densities $e = .5 - 1.4 \text{ GeV}/\text{fm}^3$, the temperature and pressure are nearly constant. Over this range then, the ratio of pressure to energy density p/e , decreases and reaches a minimum at a particular energy density known as the *softest point*, $e_{sp} \approx 1.4 \text{ GeV}/\text{fm}^3$ [8]. When the initial energy density is close to e_{sp} , the small pressure (relative to e) cannot effectively accelerate the matter. However, when the initial energy density is well above e_{sp} , p/e approaches $1/3$, and the larger pressure drives collective motion [8,9]. At a time of $\sim 1 \text{ fm}/c$, the energy densities at the SPS($\sqrt{s}_{NN} = 17 \text{ GeV}$) and RHIC ($\sqrt{s}_{NN} = 130 \text{ GeV}$) are very approximately 4 and $7 \text{ GeV}/\text{fm}^3$ respectively [10,11]. Based on these experimental estimates, the hard QGP phase is expected to live significantly longer at RHIC than at the SPS. The final flows of the produced particles should reflect this difference. In this paper we pose the question: Can both the radial and elliptic flow at the SPS and RHIC be described by a single effective EoS?

Since the various hadron species have different elastic cross sections, they freezeout (or decouple) from the hot fireball at different times [12]. Because flow builds up over time, it is essential to model this differential freezeout. It was ignored in previous hydrodynamic simulations of non-central heavy ion collisions and elliptic flow

was over-predicted flow by a factor of two [13,14].

2. The Hydro to Hadrons(H2H) model will be described in detail elsewhere [15]. Other authors have previously constructed a similar model for central collisions [16]. The model evolves the QGP and mixed phases as a relativistic fluid, but switches to a hadronic cascade (RQMDv2.4 [17]) at the beginning of the hadronic phase to model differential freezeout. The computer code consists of three distinct components. Assuming Bjorken scaling, the first component solves the equations of relativistic hydrodynamics in the transverse plane [6] and constructs a switching surface at a temperature, $T_{switch} = 160 \text{ MeV}$. The second component generates hadron on the switching surface using the Cooper-Frye formula [18] with a theta function rejecting backward going particles [19,20]. Finally, the third component (RQMD) sequentially re-scatters the generated hadrons until freezeout.

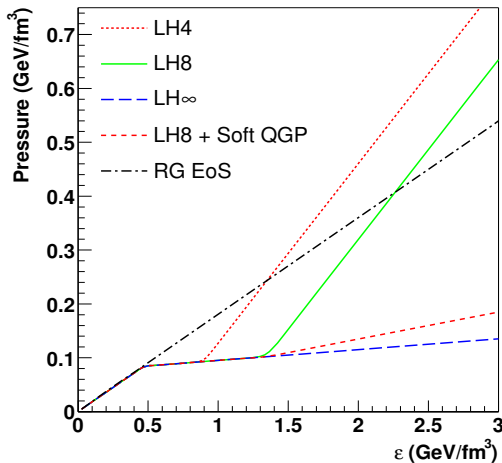


FIG. 1. The pressure versus the energy density(ϵ) for different EoSs (see text). EoSs with Latent Heats $0.4 \text{ GeV}/\text{fm}^3$, $0.8 \text{ GeV}/\text{fm}^3$,... are labeled as LH4, LH8,...

For the hydrodynamic evolution, a family of EoSs (see Fig. 1) was constructed with an adjustable Latent Heat(LH). The EoSs with latent heats $0.4 \text{ GeV}/\text{fm}^3$, $0.8 \text{ GeV}/\text{fm}^3$,... are labeled as LH4, LH8,..etc. LH ∞

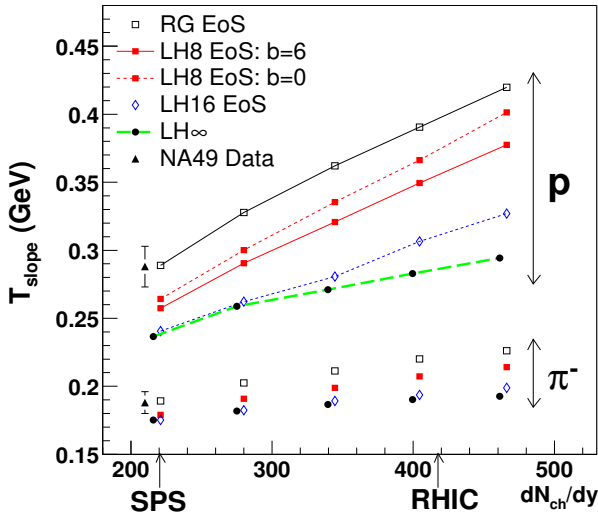


FIG. 2. The transverse mass slope(T_{slope}) as a function of the total charged particle multiplicity in PbPb collisions at an impact parameter of $b=6\text{ fm}$ (see also [9,16]). For consistency with the elliptic study in Fig. 3, we show $b=6\text{ fm}$ although the NA49 data points [21] are for $b=0\text{ fm}$. For all EoSs at the SPS, the proton slope parameters at $b=6\text{ fm}$ are $\approx 7\text{ MeV}$ smaller than at $b=0\text{ fm}$, as for the $b=0$ LH8 curve. The difference is negligible for π^- .

is considered as a limiting case, mimicking non-equilibrium phenomena [22]. The hadron phase exists up to a critical temperature of $T_c = 165\text{ MeV}$, and consists of ideal gas mixture of the meson pseudoscalar and vector nonets and the baryon octet and decuplet. The hadron phase is followed by a mixed phase with a specified LH, which is finally followed by a QGP phase with $C_s^2 = 1/3$. Since LH ∞ is slightly pathological, we compare LH ∞ to a similar EoS, LH8+Soft QGP, which has a latent heat of $0.8\text{ GeV}/\text{fm}^3$ and a slightly larger speed of sound in the quark phase, $C_s^2 = .05$. In addition, a Resonance Gas(RG) EoS was constructed with a constant speed of sound above the hadron phase.

3. *Radial flow* is quantified experimentally by slope parameters, T_{slope} ; the momentum spectrum of each particle is fit to the form $dN/dM_T^2 dy|_{y=0} = C e^{-M_T/T_{slope}}$ where $M_T^2 = P_T^2 + m^2$. T_{slope} incorporates random thermal motion and the collective transverse velocity.

In Fig. 2, the pion and proton slope parameters are plotted as functions of the total charged particle multiplicity in the collision. Look first at the leftmost points at SPS multiplicities and compare the model and experimental slopes: The proton slope data favor a relatively hard EoS – LH8 or harder. A direct comparison of the model to published spectra [23] supports this claim [15]. A RG EoS can also reproduce the proton flow. A similar analysis of elliptic flow (shown and quantified below) favors a relatively soft EoS – LH8 or softer. With some caveats, LH8 represents a happy middle which can reproduce the elliptic and radial flow at the SPS.

Look now at the energy/multiplicity dependence of the

slopes. For all EoSs, T_{slope} increases with the collision energy [9,16]. For a soft EoS (e.g. LH ∞) the increase is small and for a hard EoS (e.g. LH8) the increase is large. At RHIC multiplicities, the difference between the slope parameters is large and easily experimentally observable.

4. *Elliptic flow* is quantified experimentally with the number elliptic flow parameter, $V_2 = \langle \cos(2\Phi) \rangle$; here Φ is the angle around the beam measured relative to the impact parameter and $\langle \rangle$ denotes an average over the single particle distribution, $\frac{dN}{dP_T d\Phi}$. The momentum elliptic flow, $A_2 = \langle P_T^2 \cos(2\Phi) \rangle / \langle P_T^2 \rangle$ is also used [6]. V_2 and A_2 measure the response of the fireball to the spatial deformation of the overlap region, which is usually quantified in a Glauber model by the eccentricity, $\epsilon = \langle (y^2 - x^2) \rangle / \langle (x^2 + y^2) \rangle$ [6]. Since the response (V_2 and A_2) is proportional to the driving force (ϵ), the ratio V_2/ϵ is used to compare different impact parameters and nuclei [24,25].

In Fig. 3(a), the number elliptic flow (V_2) is plotted as a function of charged particle multiplicity at an impact parameter of 6 fm . Before studying the energy dependence, look at the magnitude of the elliptic flow at the SPS. For LH8, the stars show the pion V_2 when the matter is evolved as a fluid until a decoupling temperature of $T_f = 120\text{ MeV}$; they further illustrate the excessive elliptic flow typical of pure hydrodynamics. Once a cascade is included, LH8 (the squares) is only $\approx 20\%$ above the data – a substantial improvement. Typically in hydrodynamic calculations, the freezeout temperature T_f is adjusted to fit the proton P_T spectrum. However, protons are driven by a pion “wind” and decouple from the fireball $5\text{ fm}/c$ after the pions on average. This pion wind accounts for the strong proton flow at the SPS and is certainly not described by ideal hydrodynamics [16,15]. In order to match the observed proton flow, hydrodynamic calculations must decouple at low freezeout temperatures, $T_{frz} \approx 120\text{ MeV}/c$. Decoupling at low temperatures has three consequences for elliptic flow: First the reduction of elliptic flow due to resonance decays is small $\approx 15\%$, compared to $\approx 30\%$ in the H2H model. Second, compared to a cascade, the hydrodynamics generates twice as much elliptic flow during the late cool hadronic stages of the evolution. Third, the elliptic flow is not reduced by random thermal motion. By including the pion “wind”, and more generally by decoupling differentially, we can simultaneously describe the radial and elliptic flow data at the SPS.

The energy dependence of V_2 is the central issue. As seen in Fig. 3, the H2H model predicts an increase in elliptic flow by a factor ≈ 1.4 and is in reasonable agreement with SPS and RHIC flow data. This result was presented prior to the publication of RHIC data [20]. In contrast, UrQMD, a hadronic cascade based on string dynamics, predicts a decrease by a factor of ≈ 2 [26]. This is because the UrQMD string model has a Hagedorn limiting temperature, resulting in a super-soft EoS at high energies [27]. For pure hydrodynamics as illustrated by

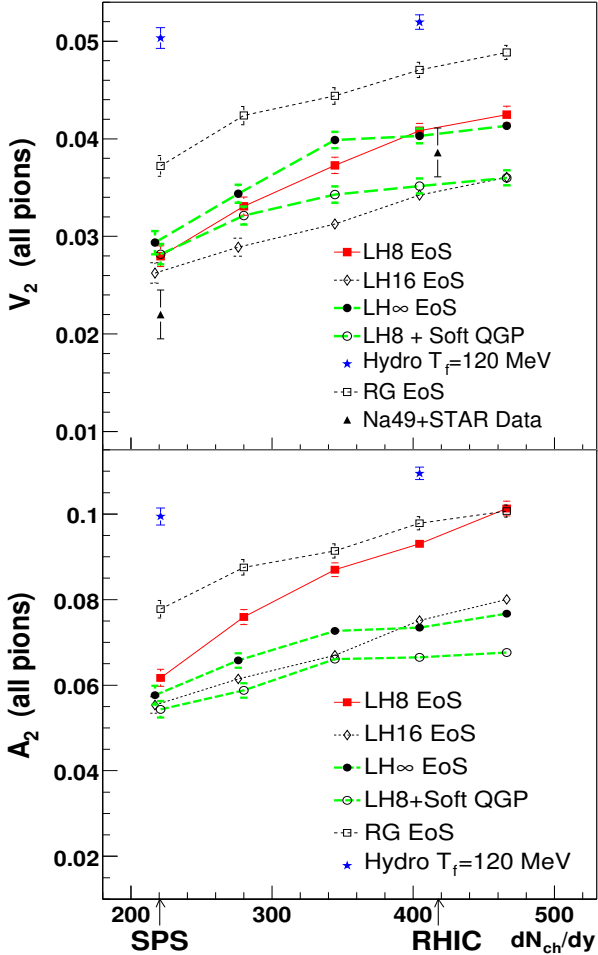


FIG. 3. (a) The number elliptic flow parameter V_2 , and (b) The momentum elliptic flow parameter A_2 , as a function of the charged particle multiplicity in PbPb collisions at an impact parameter of $b=6$ fm. (a) At the SPS, the NA49 V_2 data point is extrapolated to $b=6$ fm using Fig. 3 in [4]. At RHIC, the STAR V_2 data point is extrapolated to $N_{ch}/N_{ch}^{max} = 0.545$ ($b=6$ fm in AuAu) using Fig. 3 in [5]. The comparison to data is a little unfair: For the model, V_2 is calculated using all pions in PbPb collisions. For the NA49 data, V_2 is measured using only π^- in PbPb (a -3% correction to the model). For the STAR data, V_2 is measured using charged hadrons in AuAu (a +5% correction to the model).

the stars, V_2 is approximately constant [13] (but see [14]). For HIJING [28], a model which considers only the initial parton collisions, V_2 is ≈ 0 [29]. The first RHIC data clearly contradict these models.

The increase in V_2 is now used to constrain the EoS of the excited matter. The QCD phase diagram has two distinguishing features. It is soft at low energy densities and subsequently hard at high energies. A RG EoS (the open squares) has no softness and the elliptic flow is clearly too strong both at the SPS and RHIC. The entire family of EoSs, LH8 through LH ∞ , reproduces the elliptic flow data in both energy regimes. Counter-intuitively, as the

latent heat is increased V_2 first decreases and then increases. In the final count, LH8 and LH ∞ have roughly the same V_2 . However, they correspond to two very different hydrodynamic solutions. For LH8, the EoS shifts from hard to soft and the matter explodes, forming two shells of outgoing matter [30]. For LH ∞ , the EoS is just soft and the matter burns slowly inward, evaporating particles into RQMD. For LH ∞ the fireball lives a long time [8] and this is responsible for the significant V_2 . At RHIC, the fireball lifetime for LH ∞ is ≈ 16 fm/c in contrast to ≈ 9 fm/c for LH8. For LH ∞ , V_2 builds up slowly but the driving force, the spatial asymmetry ϵ , is only slowly destroyed. Over the long lifetime of the system, the driving force is slowly integrated, and the very soft EoS builds up a large V_2 . Since LH ∞ (the closed circles) is slightly pathological, we compare it to LH8+Soft QGP (the open circles), which has a small speed of sound and which builds up just a little transverse motion. As seen in Fig. 3(a), even a little transverse motion reduces the lifetime and V_2 of LH ∞ significantly.

The difference between the LH8 and LH ∞ is further clarified in Fig. 3(b) by plotting the momentum elliptic flow, A_2 . A_2 increases rapidly for LH8 and levels off for LH ∞ . Thus, the super soft EoS LH ∞ generates number elliptic flow V_2 , but not momentum elliptic flow, A_2 . Eventually pressure wins over lifetime and LH8 produces a larger V_2 and A_2 than LH ∞ . The P_T dependence of V_2 did not discriminate between LH8 and LH ∞ and both EoSs agreed with the STAR data within experimental errors [15]. For both EoSs, the pressure, is greater than $p_c \approx 75$ MeV/fm 3 during the initial phases. Therefore, the current STAR data, while not conclusively signaling the asymptotic pressure in the QGP, does indicate a substantial degree of equilibration for energy densities larger than $e_c \approx 0.4$ GeV/fm 3 .

5. Impact Parameter Dependence. In Fig. 4, V_2 for LH8 as a function of the number participants(N_p) is compared to data. Different EoSs show a similar participant (or b) dependence. The agreement is good at RHIC where the multiplicity is high. For ideal hydrodynamics, $V_2 \propto \epsilon \propto (N_p^{max} - N_p)$ [6]. In the low density limit, since the response is proportional to the number of collisions, $V_2 \propto \epsilon \frac{dN}{dy} \propto (N_p^{max} - N_p)N_p$. Therefore, V_2 has a different N_p (or b) dependence in the hydrodynamic and low density limits [24,25]. At RHIC, except in very peripheral collisions, the N_p dependence is clearly linear and strongly supports the hydrodynamic limit [5]. At the SPS, the N_p dependence may not be clearly linear, but it also does not follow the low density limit. Two-pion correlations, may change the data analysis [31], reduce the elliptic flow in peripheral collisions, and improve the low density agreement. Working against the low density limit, the rapidity dependence of V_2 [4] does not follow the $\frac{dN}{dy}$ multiplicity distribution as might naively be expected. Estimates based on the low density limit do correctly predict an increase in V_2 with energy/multiplicity [25]. However, given the reasonable success of the current

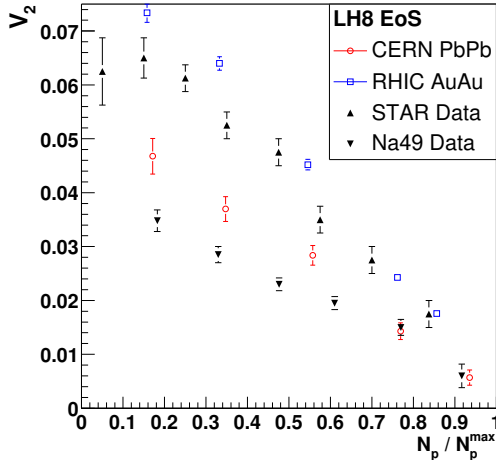


FIG. 4. V_2 versus the number of participants(N_p) relative to the maximum . The model and the NA49 V_2 values [4] at the SPS are for π^- . The NA49 data are mapped from b to participants using [32]. The model and the STAR V_2 values [5] at RHIC are for charged particles. The model does not include weak decays. The number of charged particles is assumed proportional to N_p .

model, it may be premature to conclude that the early evolution at the SPS is not hydrodynamic.

6. Summary and Discussion. By incorporating differential freezeout, the Hydro to Hadrons(H2H) model simultaneously reproduces the radial and elliptic flow at the SPS and RHIC. At the SPS, the radial flow demands an EoS with a latent heat $LH \gtrsim 0.8 \text{ GeV}/\text{fm}^3$, while elliptic flow demands an EoS with a latent heat $LH \lesssim 0.8 \text{ GeV}/\text{fm}^3$. Further, in contrast to string and collision-less parton models, the increase in V_2 is naturally explained using hydrodynamics. This challenges the prevailing view [5,25] that the SPS is in the low density regime and that the increase in V_2 represents a transition to the hydrodynamic regime. However, the increase in V_2 does not uniquely signal the asymptotic QGP pressure. Indeed, at RHIC collision energies, a very soft EoS can have the same V_2 as an EoS with a well developed QGP phase. This EoS is not academic since softness can mimic non-equilibrium phenomena [22].

To reveal the underlying EoS and the burgeoning QGP pressure, the collision energy should be scanned from the SPS to RHIC. If the prevailing low density view of the SPS is correct, a transition in the b dependence of elliptic flow should be observed over the energy range [24,25]. In addition, V_2 and especially A_2 have a different collision energy dependence for different EoSs (Fig. 3). Taken with the radial flow (Fig. 2), this experimental information would help settle the EoS of hot hadronic matter.

Acknowledgments The work is partly supported by the US DOE grant No. DE-FG02-88ER40388.

- [1] e.g., E.V. Shuryak, Phys. Rept. **61**, 71 (1980); L. McLerran , Rev. Mod. Phys. **58**, 1021 (1986).
- [2] e.g., R. Stock, in QM '99 , Nucl. Phys. **A661**, 419c (1999).
- [3] e.g., E895 Collaboration, C. Pinkenburg *et al.* Phys. Rev. Lett. **83**, 1295 (1999); NA49 Collaboration, H. Appelshäuser *et al.*, Phys. Rev. Lett. **80**, 4136 (1998); see also QM '99 Nucl. Phys. **A661**(1999).
- [4] A.M. Poskanzer and S.A. Voloshin for the NA49 Collaboration, Nucl. Phys. **A661**, 341c (1999).
- [5] STAR Collaboration, K.H. Ackermann *et al.* ; nucl-ex/0009011.
- [6] J.-Y. Ollitrault, Phys. Rev. **D46**, 229 (1992)
- [7] e.g., M. Oevers, F. Karsch, E. Laermann, and P. Schmidt, Nucl. Phys. Proc. Suppl. **73**, 465 (1999).
- [8] C.M. Hung, E.V. Shuryak, Phys. Rev. Lett. **75**, 4003 (1995); D. H. Rischke and M. Gyulassy, Nucl. Phys. **A608**, 479 (1996).
- [9] M. Kataja *et al.*, Phys. Rev. **D34**, 794 and 2755 (1986).
- [10] NA49 Collaboration, T. Alber *et al.*, Phys. Rev. Lett. **75**, 3814 (1995).
- [11] PHOBOS Collaboration, B.B. Back *et al*, Phys. Rev. Lett. **85**, 3100 (2000) ; hep-ex/0007036
- [12] H. Sorge, Phys. Rev. Lett. **81**, 5764 (1998).
- [13] P. Kolb, J. Sollfrank, U. Heinz, Phys. Lett. **B459**, 667 (1999).
- [14] P. Kolb, J. Sollfrank, U. Heinz, preprint hep-ph/0006129.
- [15] D. Teaney, J. Lauret, and E.V. Shuryak, in progress.
- [16] S. Bass and A. Dumitru, Phys. Rev. **C61**, 064909 (2000).
- [17] H. Sorge, Phys. Rev. **C 52**, 3291 (1995).
- [18] F. Cooper and G. Frye, Phys. Rev. **D10**, 186 (1974)
- [19] For discussion see, Cs. Anderlik *et al.*, Phys. Rev. **C59**, 388 (1999) and references therein.
- [20] qualitatively, E.V. Shuryak in QM '99 , Nucl. Phys. **A661**, 119c (1999); quantitatively, D. Teaney *et al.*, talk at RHIC2000, Park City, Utah, March 10-15 (2000); <http://theo8.nscl.msu.edu/RHIC2k/proceedings.htm>.
- [21] G. Roland for the NA49 Collaboration, Nucl. Phys. **A638**, 91c (1999).
- [22] H. Sorge, Phys. Lett. **B402**, 251 (1997).
- [23] NA49 Collaboration, H. Appelshäuser *et al.*, Phys. Rev. Lett. **82**, 2471 (1999).
- [24] H. Heiselberg and A.-M. Levy, Phys. Rev. **C59**, 2716 (1999).
- [25] S.A. Voloshin and A.M. Poskanzer, Phys. Lett. **B474**, 27 (2000).
- [26] M. Bleicher and H. Stocker, preprint hep-ph/0006147.
- [27] M. Belacem *et al.*, Phys. Rev. **C58**, 1727 (1998).
- [28] M. Gyulassy and X.N. Wang, Comp. Phys. Comm. **83**, 307 (1994); Phys. Rev. **D44**, 3501 (1991).
- [29] R.J.M Snellings, A.M. Poskanzer, S.A. Voloshin, STAR Note SN0388 (1999), preprint nucl-ex/9904003.
- [30] D. Teaney and E.V. Shuryak, Phys. Rev. Lett. **83**, 4951 (1999).
- [31] P.M. Dinh, N. Borghini, and J.-Y. Ollitrault, Phys. Lett. **B477**, 51 (2000); N. Borghini, P.M. Dinh, and J.-Y. Ollitrault, Phys. Rev. **C62**, 34902 (2000); For a new data analysis method see: N. Borghini, P.M. Dinh, and J.-Y. Ollitrault, nucl-th/0007063.
- [32] G. Cooper for the NA49 Collaboration, Nucl. Phys. **A661**, 362c (1999).